A NOVEL ESTIMATION SYSTEM FOR MULTIPLE PULSE ECHO SIGNALS FROM ULTRASOUND CONTRAST MICROBUBBLES

Yan Yan, James R.Hopgood and Vassilis Sboros *

Institute for Digital Communications,
School of Engineering and Electronics, University of Edinburgh, UK
{Y.Yan@ed.ac.uk, James.Hopgood@ed.ac.uk and vassilis.sboros@ed.ac.uk}

ABSTRACT

The understanding and exploitation of non-linear microbubble signals is an active research area that aims to advance contrast ultrasound into a high sensitivity and specificity diagnostic imaging modality. To discriminate the difference between echoes from tissue and contrast microbubbles, it is of significance to extract as much information of the reflected signals as possible, especially the pulse locations in the time domain and their corresponding spectral contents in the frequency domain. In this paper, a novel estimation system for extracting the information of interest is proposed. This estimation technique is based on non-parametric methods for coarse estimation, followed by a parametric method within Bayesian framework for estimation refinement. The results show that the pulse location and frequency content can be accurately estimated simultaneously. This assists in the design of transmit pulsing regimes in future work.

***Index Terms*—** ultrasound contrast microbubbles, Bayesian inference, Monte Carlo methods, parametric model

1. INTRODUCTION

Microbubbles have been widely used as Ultrasound Contrast Agents (UCAs) in bio-medical research area since the 1990's [1]. They are composed of gas-filled encapsulated microspheres, usually with diameter below $7\mu m$, that can go through microcirculations in the human body. The microbubbles have a non-linear acoustic signature, as they are more compressible when exposed to an oscillating acoustic signal compared to soft tissue [2]. In order to design a transmit pulse that can maximise the difference between responses from microbubbles and tissue and increase the contrast-to-tissue ratio (CTR) [3], it is of particular interest to jointly extract the characteristics of responses in both the time and frequency domains.

Most traditional methods for frequency estimation in ultrasound are based on the Fourier transform (FT) methods [3]. However, due to the limitations of frequency resolution, the FT can not detect some frequencies that may have important physical meanings, or may provide false spectral contents. Moreover, it does not localize in time. Additionally, in the time domain, pulse locations and durations attract more attention. The Hilbert transform [4] is widely used for envelope detection. It may fail when the signal is embedded in noise. Moreover, it only operates in the time domain and cannot offer any frequency information about the signal. There is little information in the ultrasonic literature about the joint estimation of pulse locations and frequencies, which can be further developed, especially for multiple pulse echo signals.

In this paper, a new ultrasound contrast microbubble estimation system is proposed. The whole procedure is outlined in section 2. In section 3, coarse estimation for pulse locations and spectral content based on nonparametric methods is described. In section 4, optimisation of parameters using a parametric model within the Bayesian framework provides more accurate estimates. Performance evaluation for the synthetic signals and experimental signals are both shown in section 5. Section 6 concludes that the proposed estimation system can extract the information in both time and frequency domains simultaneously.

2. ULTRASOUND CONTRAST MICROBUBBLE ESTIMATION SYSTEM

The design of a complete estimation system is required to extract the information of echo signals from microbubbles automatically. The system can be divided into two parts, as displayed in Fig.1. The first part is coarse estimation for pulse locations and the frequency contents; the second part is to refine the estimation by using a parametric model within Bayesian framework. Details are described later in sections 3 and 4.

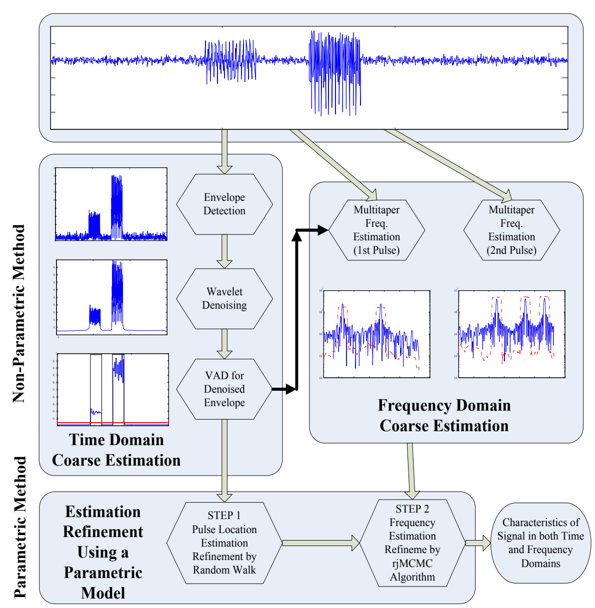

Fig. 1. Procedure for the whole estimation system

*Vassilis Sboros is with Department of Medical Physics. IDCOM is in the Joint Research Institute for Signal and Image Processing, a member of the Edinburgh Research Partnership in Engineering and Mathematics. This project is funded by Biologically Inspired Acoustic System (BIAS).

3. COARSE ESTIMATION

3.1. Coarse Estimation in Time Domain

From the observation of responses from microbubbles, the techniques used for signal burst detection can be applied to pulse location estimation of the microbubble echo signals in ultrasound imaging. The estimation of pulse location is related to the estimation of the start and end points of each pulse.

3.1.1. Wavelet Denoising for Envelope Detection

Envelope detection using the Hilbert transform is widely used for changepoints (start and end points) estimation [4]. In the case of low signal-to-noise ratio(SNR), the envelope detected by the Hilbert transform is quite noisy, thus can not be easily extracted. In order to obtain a clearer envelope of the multiple pulse signal, wavelet denoising is adopted as it has more advantages compared with traditional filtering approaches, e.g. it is non-linear and can be applied to non-stationary signals. However, the method may fail when there are closely-spaced pulses present in the real bubble signal.

3.1.2. Voice Activity Detection

Voice activity detection (VAD) is an energy detector in various applications. The technique used by Alan [5] introduces a low-variance spectral estimator and determines an optimal threshold based on the estimated noise statistics. Nevertheless, if the SNR of the signal is low or the amplitudes of microbubble pulses are small, the performance of VAD is not acceptable since the threshold may not be properly chosen.

3.1.3. Coarse Estimation of Pulse Location

Although both the VAD algorithm and wavelet denoising for envelope detection have their own limitations, the combination of these two can improve the detection accuracy. Firstly, the Hilbert transform is used for envelope detection. Secondly, the envelope is denoised by a stationary wavelet transform, which is selected for its time-invariant property [6]. Finally, the VAD algorithm is performed for the denoised envelope. Following the aforementioned procedure of the algorithm, the proposed method can give better estimation for both closely-spaced pulses and small amplitude pulses. In addition, by experimental observation, the method can tolerate lower SNR down to $5dB$.

3.2. Coarse Estimation in Frequency Domain

The discrete Fourier transform (DFT) is often used to analyze the signal in the frequency domain. Andrieu and Doucet proposed a frequency estimation algorithm based on the DFT in [7]. This approach can sometimes overestimate the number of frequencies. Therefore, the multitaper spectral estimator is introduced to refine the sampling process in the algorithm. In this technique, several data windows are used on the same data record to obtain several modified periodograms. These periodograms are then averaged to produce the multitaper spectrum [8]. By reducing the variance, a much cleaner spectrum is achieved. Moreover, the bias and resolution loss can also be reduced for properly designed tapers.

4. ESTIMATION REFINEMENT

The aforementioned estimation techniques are all non-parametric methods, which can only provide coarse estimation of the parameters of interest. Furthermore, for frequency estimation, multitaper spectral estimator only works for one specific segment of pulse and cannot offer the number of frequencies automatically. When there are multiple pulses in the signal and the number of frequencies for each pulse is unknown, more advanced techniques, such as using a parametric model within Bayesian framework, can give more accurate estimates.

4.1. Signal Model

As the experimental transmit pulse in ultrasound appears to be composed of several cycles of a harmonic signal, the multiple pulse bubble echo can be modeled as several segments of sum of sinusoids. Assume there are m pulses in the observed signal with N data points. The multiple pulses model can be defined as follows: ($T_0 \triangleq 1$, $T_{2m+1} \triangleq N$ and $i = 0, \dots, 2m$)

$$\begin{aligned} D_0 &: \quad x(t) = n(t) \\ D_{k_m} &: \quad x(t) = \begin{cases} n(t) & \text{if } T_i < t \leq T_{i+1} - 1, \, i \text{ is even} \\ x_i(t) + n(t) & \text{if } T_i < t \leq T_{i+1} - 1, \, i \text{ is odd} \end{cases} \end{aligned}$$

where $x_i(t) = \sum_{j=1}^{k_i} a_{c_{j,k_i}} \cos(\omega_{j,k_i} t) + a_{s_j,k_i} \sin(\omega_{j,k_i} t)$.

The signal model can be written in a vector-matrix form:

$$\mathbf{x} = \mathbf{G}(\boldsymbol{\omega}_{k_m}, \boldsymbol{T}_{2m})\mathbf{a}_k + \mathbf{n} \tag{1}$$

where $\mathbf{n}$ is the zero-mean white Gaussian noise with variance σ_k^2 and

$$\mathbf{G} = \begin{bmatrix} 0 & 0 & \cdots & 0 \\ \boldsymbol{G}_1 & 0 & \cdots & 0 \\ 0 & 0 & \cdots & 0 \\ 0 & \boldsymbol{G}_2 & \cdots & 0 \\ 0 & 0 & \cdots & 0 \\ \vdots & \vdots & \ddots & \vdots \\ 0 & 0 & \cdots & 0 \\ 0 & 0 & \cdots & \boldsymbol{G}_m \\ 0 & 0 & \cdots & 0 \end{bmatrix}.$$

The $\mathbf{G}$ matrix is of size $2N \times \sum_{i=1}^{m} k_i$. It contains the information about changepoints $(T_1, T_2, \dots, T_{2m})$, which are related to the positions of multiple pulses in the echo signal. Each component $\boldsymbol{G}_j (j = 1, \dots, m)$ in $\mathbf{G}$ matrix represents a single pulse, which has its own parameters. The number of sinusoids and other parameters $\boldsymbol{\theta}_k \triangleq (\boldsymbol{\omega}_k, \boldsymbol{a}_k, \sigma_k^2)$ are all unknown in each pulse. As far as each segment is concerned, the $\boldsymbol{G}_j$ matrix can be defined as:

$$\boldsymbol{G_j} = \begin{bmatrix} E(\omega_{k_1} t(T_{2j-1})) & \dots & E(\omega_{k_m} t(T_{2j-1})) \\ E(\omega_{k_1} t(T_{2j-1} + 1)) & \dots & E(\omega_{k_m} t(T_{2j-1} + 1)) \\ \vdots & \vdots & \vdots \\ E(\omega_{k_1} t(T_{2j} - 1)) & \dots & E(\omega_{k_m} t(T_{2j} - 1)) \end{bmatrix}$$

where $E(\cdot) \triangleq [\cos(\cdot), \sin(\cdot)]$. Moreover, T_{2j-1} and T_{2j} are two corresponding changepoints at the start and end points respectively for each pulse segment. For each $\boldsymbol{G}_j$, k_m may have different values, which implies the different number of frequencies and their values in different pulses.

The likelihood function can be easily obtained according to the signal model (m in $\{k, \boldsymbol{\theta}_k\}_m$ represents different pulse segment):

$$p(\mathbf{x}|\{k, \boldsymbol{\theta}_k\}_m, \boldsymbol{T}_{2m}) = (2\pi\sigma_k^2)^{-N/2} \times \exp\left\{ -\frac{1}{2\sigma_k^2} \parallel \mathbf{x} - \mathbf{G}(\boldsymbol{\omega}_{k_m}, \boldsymbol{T}_{2m})\boldsymbol{a}_k \parallel^2 \right\}. \tag{2}$$

4.2. Reversible jump MCMC Algorithm for Frequency Estimation Refinement

According to Bayesian inference [9], the joint posterior distribution is achieved based on the properly chosen prior distribution of all the parameters. The joint prior distribution and the posterior distribution, after integrating out the nuisance parameters $\boldsymbol{a}_{k_m}$ and σ_k^2, are expressed as follows (more details can be found in [7] and v_0, γ_0, Λ, δ^2 are hyperparameters of the Bayesian model):

$$\begin{aligned} p(\{k,\boldsymbol{\theta}_k\}_m, \boldsymbol{T}_{2m}) &= p(\boldsymbol{T}_{2m})p(\{k,\boldsymbol{a}_k,\boldsymbol{\omega}_k\}_m|\sigma_k^2)p(\sigma_k^2) \\ &\propto \frac{\Lambda^{k_m}}{k_m!}\exp(-\Lambda) \times \frac{1}{|2\pi\sigma_k^2\Sigma_{k_m}|^{1/2}} \times \frac{1}{\pi^{k_m}}\frac{1}{\sigma_k^2} \\ &\times \exp[-\frac{\boldsymbol{a}_{k_m}^T\Sigma_{k_m}^{-1}\boldsymbol{a}_{k_m}}{2\sigma_k^2}] \times (\frac{1}{N-1}\frac{1}{N-2}\cdots\frac{1}{N-2m}) \end{aligned} \quad (3)$$

where $\Sigma_{k_m}^{-1} = \delta^{-2}\mathbf{G}^T(\boldsymbol{\omega}_{k_m}, \boldsymbol{T}_{2m})\mathbf{G}(\boldsymbol{\omega}_{k_m}, \boldsymbol{T}_{2m})$.

$$p(\boldsymbol{T}_{2m}, \{k,\boldsymbol{\omega}_k\}_m|\mathbf{x}) \propto (\gamma_0 + \mathbf{x}^T\mathbf{P}_{k_m}\mathbf{x})^{-(N+v_0)/2} \times \frac{(\Lambda/[(\delta^2+1)\pi])^{k_m}}{k_m!} \quad (4)$$

where $\mathbf{P}_{k_m} = \mathbf{I}_N - \mathbf{G}(\boldsymbol{\omega}_{k_m}, \boldsymbol{T}_{2m})\mathbf{M}_{k_m}\mathbf{G}^T(\boldsymbol{\omega}_{k_m}, \boldsymbol{T}_{2m})$, $\mathbf{I}_N$ is a $N\times N$ identity matrix and $\mathbf{M}_{k_m}^{-1} = \mathbf{G}^T(\boldsymbol{\omega}_{k_m}, \boldsymbol{T}_{2m})\mathbf{G}(\boldsymbol{\omega}_{k_m}, \boldsymbol{T}_{2m}) + \Sigma_{k_m}^{-1}$.

However, the joint posterior distribution is highly non-linear, which means the closed form of $p(\boldsymbol{T}_{2m}, \{k,\boldsymbol{\omega}_k\}_m|\mathbf{x})$ can not be obtained. Therefore, a reversible jump Markov chain Monte Carlo (rjMCMC) algorithm is introduced to sample from the complicated joint distribution and then to estimate the multiple pulse locations and frequency contents for each pulse simultaneously.

In the proposed algorithm, a multitaper spectrum is adopted as the proposal distribution to provide the initial guess for frequency estimation. The rjMCMC algorithm is then used to explore the regions around obvious peaks in the multitaper power spectrum. Furthermore, as the number of frequencies and their values are all unknown, the reversible jump MCMC technique is incorporated to select the model order of the frequency automatically.

4.3. Random Walk Update for Pulse Locations

Based on the initial guesses given by aforementioned combination algorithm of VAD and wavelet denoising for envelope detection, a random walk perturbation is adopted as the proposal distribution for refinement of the pulse location estimates. Specifically, the update of each changepoint depends on its previous value and performs a local exploration of the initial guess, which can be described as:

$$T^*|T \sim \mathcal{N}(T, \sigma_T^2). \quad (5)$$

where T and T^* are previous state and new state of the changepoint respectively. $\mathcal{N}(\cdot)$ represents the normal distribution with mean T and variance σ_T^2.

4.4. Refinement Algorithm Based on a Parametric Model

The refinement of the parameter estimates, for both pulse location and frequency content, using a parametric model with numerical Bayesian method, consists of two steps in each iteration. Firstly, the pulse locations are updated by random walk perturbation; secondly, after the estimation of pulse locations, frequency contents for each pulse can be updated using rjMCMC algorithm for a given specific set of changepoints. The procedure is summarized in Algorithm 1. Details of the birth, death and update moves can be found in [7].

Algorithm 1 rjMCMC Algorithm for Estimation Refinement

Initialization: set $(\{k,\boldsymbol{\theta}_k\}_m^{(0)}, \boldsymbol{T}_{2m}^{(0)})$.
Iteration:
for $i = 1$ to $numIteration$ **do**
    Update each changepoint $\boldsymbol{T}_{2m}^{(i)}$ using random walk.
    For each pulse segment m, update frequency contents:
    a).Sample hyperparameters Λ and δ^2.
    b).Sample u from $U_{(0,1)}$. (*uniform distribution*)
    if $u \leq b_{k_m^{(i)}}$ **then**
        perform *birth move* of a new frequency
    else if ($u \leq b_{k_m^{(i)}} + d_{k_m^{(i)}}$) **then**
        perform *death move* of an existing frequency
    else
        perform *update move* of a frequency randomly
    end if
    c).Sample nuisance parameters $\boldsymbol{a}_{k_m}$ and σ_k^2.
end for

Table 1. Comparison of Accuracy between Coarse Estimation and Estimation Refinement of Pulse Locations (start & end points) SNR = 5dB

True Locations	450	600	750	900
Coarse Estimation	460	600	780	890
$\mid \triangle\varepsilon \mid$	10	0	20	10
Estimation Refinement	448	598	750	900
$\mid \triangle\varepsilon \mid$	2	2	0	0

5. RESULTS AND EVALUATION

5.1. Evaluate the Estimation System on Synthetic Signals

According to the characteristics of the multiple pulse echo signal from ultrasound contrast microbubbles, the synthetic signal is simulated as several pulse segments with a sum of sinusoids in each segment. This synthetic signal is used to evaluate the performance of the whole estimation system.

The synthetic signal has 1500 data points, which consists of two pulses. The first pulse locates between (450, 600) and has two frequency components ($0.2\pi = 0.6283$, $0.6\pi = 1.8849$); the second one locates between (750, 900) and has three frequencies ($0.4\pi = 1.2566$, $0.8\pi = 2.5132$, $0.3\pi = 0.9425$). After the estimation procedure, the coarse estimation and the estimation refinement for pulse locations are compared in Table 1. The error is calculated as the sum of difference between true values and estimated values of each pulse location. The error after estimation refinement is much less than that of coarse estimation only. Moreover, the frequency contents can be estimated at the same time with high accuracy {(0.6288, 1.8846); (1.2560, 2.5130, 0.9433)} compared to multitaper estimation { (0.6250, 1.8860); (1.2552, 2.5145, 0.9440) }.

Furthermore, the above experiments has been repeated 100 times with different noise realizations and amplitudes and phase components. On average, the error of coarse estimation for pulse locations is 20 whereas the error after estimation refinement is 5. For frequency estimation, the error percentage of multitaper technique is around 1% and the error percentage of rjMCMC algorithm is about 0.01%. As a result, the new estimation system indicates its superi-

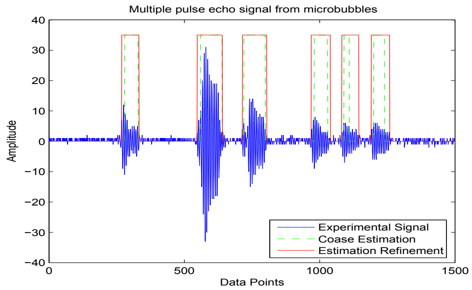

Fig. 2. Multiple pulses signal with pulse location estimation

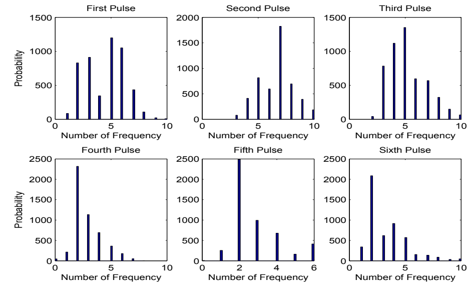

Fig. 4. Histogram of number of frequencies for each pulse segment

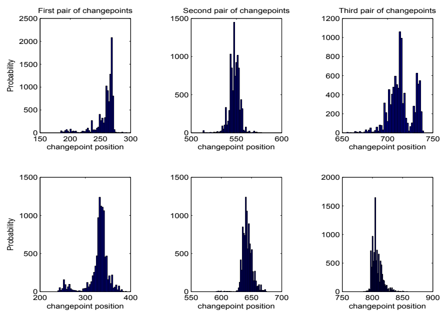

Fig. 3. Histogram of pulse locations for the first three pulses

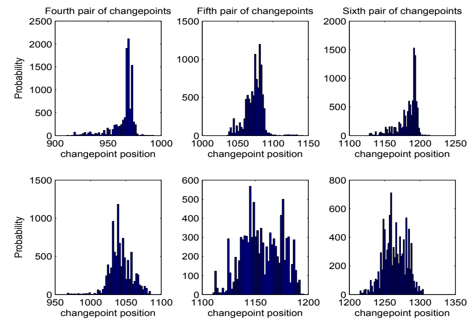

Fig. 5. Histogram of pulse locations for the last three pulses

ority in both the time domain and frequency domain.

5.2. Experimental Signal Analysis

In the following experiments, the microbubbles used for analysis in this paper are "Definity " [10], which are exposed to ultrasound peak negative pressure of 300kPa and transmit frequencies ranging from 1.1MHz to 3.2MHz. The raw signals produced from the microbubbles were preamplified, collected and stored. The multiple pulse signal shown in Fig.2 was collected with peak negative pressure of 300kPa and transmit frequency of 1.48MHz. Fig.3 and Fig.5 show histograms of the probability of pulse locations after estimation refinement $\{(269, 333), (548, 641), (715, 805), (969, 1040), (1082, 1145), (1191, 1259)\}$. The estimation result is also shown in Fig.2, denoting the locations for six pulses: The dash line represents the coarse estimation for pulse locations and the solid line represents the pulse location estimation after refinement, which offers more accurate estimates. For frequency estimation, Fig.4 depicts the histogram of number of frequency components in each pulse:(5, 7, 5, 2, 2, 2).

The whole algorithm has been carried out for other available data sets. The investigation indicates that the proposed estimation system can estimate the number of pulses in the signal and their positions, as well as the number of frequencies in each pulse and their corresponding values with very small errors simultaneously.

6. CONCLUSIONS

This paper proposes a novel estimation system for echo signals from ultrasound contrast microbubbles. The system first obtains coarse estimation by using non-parametric methods and then optimises the estimation by incorporating a parametric model within a Bayesian framework. The advantage is that it allows an automatic estimation of frequencies for each pulse and the pulse locations at the same time. Moreover, it exhibits improved frequency resolution compared to the Fourier analysis based techniques. Additionally, the parametric model introduced in the paper optimises the estimation of all parameters of interest. As a result, the new estimation system reveals more attributes in both time and frequency domains, which may broaden the research field in ultrasound contrast agents, especially in design of transmit pulsing regimes.

7. REFERENCES

[1] Gramiak R et al, "Echocardiography of the aortic root," *Invest Radio*, vol. 3, no. 356-366, 1968.

[2] E.Stride et al, "Microbubble ultrasound contrast agents, a review," *Eng. in Medicine*, vol. 217, 2003.

[3] Burns P.N. et al, "Higher harmonics of vibrating gas filled microspheres, part one, simulations," *Ultrasonics*, vol. 32, no. 447-453, 1994.

[4] Xander A et al, "Baseband velocity estimation for second-harmonic signals exploiting the invariance of the doppler equation," *IEEE Trans. on Bimedical Engineering*, vol. 45, no. 10, October 1998.

[5] A.Davis et al, "Statistical voice activity detection using low-variance spectrum estimation and an adaptive threshold," *IEEE Trans. on Speech and Audio Processing*, vol. 14, pp. 412–424, March 2006.

[6] X. Lu et al, "Removal of noise by wavelet method to generate high quality temporal data of terrestrial MODIS products," *Photogram. Eng. & Remote Sensing*, vol. 73, October 2007.

[7] C. Andrieu and A. Doucet, "Joint model selection and estimation of noisy sinusoids via reversible jump MCMC," *IEEE Trans. on Signal Processing*, vol. 47, no. 10, October 1999.

[8] D. G.Manolakis, V. K.Ingle, and S. M.Kogon, *Statistical and adaptive signal processing:Spectral estimation, signal modelling, adaptive filtering and array processing*, McGrawHill, 1st edition, August 2003.

[9] P.C.Gregory, "A bayesian revolution in spectral analysis," in *Bayesian inference and maximum entropy methods in science and engineering*. Amer.Inst.of Physics Proceedings, 2001, pp. 557–568.

[10] V.Sboros et al, "The measurement of backscatter from individual contrast agent microbubbles," in *Ultrasonic Symposium*. IEEE, 2002, pp. 1945–1947.